The Optimal Allocation Method for Energy Storage in Low Voltage Distribution Power Network

Lin Zhu[1], Xiaofang Meng[2], Nannan Zhang[3]*
College of Information and Electrical Engineering, Shenyang Agricultural University, Shenyang, China[1, 2, 3]
Anshan Power Supply Company of State Grid, Anshan, 114003, China[1]

***Abstract*—In order to promote the absorption of photovoltaic in low-voltage distribution network, and reduce the voltage over-limit problem caused by high proportion of distributed photovoltaics, this paper proposes a method for optimizing the allocation of distributed energy storage system in low voltage distribution network. Firstly, based on the node voltage of the maximum load day and all day, the optimal clustering number *k* is obtained by the elbow method, and the *K*-means clustering algorithm is used to realize the zoning of the distribution network. Secondly, the objective function is to improve the node voltage, reduce the power loss, and minimize the comprehensive cost of energy storage investment, and at the same time consider various constraints such as power balance and energy storage battery, and construct a multi-objective optimization model for the optimal configuration of distributed energy storage system in low voltage distribution network. After normalizing each objective function, the weight coefficient of each objective function is determined based on the analytic hierarchy method. The whale algorithm is used to solve the model to determine the best installation location and capacity of distributed energy storage. Finally, taking an actual area as an example, the effectiveness of the proposed model in leveling the voltage exceeding of low voltage distribution network nodes is verified.**

***Keywords*—Optimal allocation; voltage over-limit; distributed energy storage; low voltage distribution networks**

I. INTRODUCTION

Under the background of the "safe, efficient and low-carbon" Energy development strategy, it has become a development trend to raise a large amount of Distributed Photovoltaic (DPV) and Distributed Energy Storage (DES) in the distribution network [1, 2]. The increasing proportion of DPV connected to Low-Voltage Distribution Network (LVDN) will worsen the mismatch between the volatility and load characteristics of photovoltaic power and results in serious power back flow phenomenon. The reverse power flow leads to the increase of node voltage, the over-limit of node voltage, aggravates voltage fluctuation and other problems, which affects the stable operation of the distribution network [3]. With the increasing permeability of DPV in LVDN, the over-voltage problem has affected LVDN's absorption of high-proportion distributed PV [4, 5], which brings great challenges to the safe operation of the distribution network.

It is an effective way to apply DES to suppress/solve the voltage over-limit caused by the high proportion of photovoltaic in the distribution network [6-9]. The access location and capacity of Distributed Energy Storage System (DESS) directly affect the voltage quality and operation economy of the distribution network. Therefore, reasonable allocation of DES has become an urgent issue to be studied considering the voltage off-limit treatment of distribution network [10].

Many scholars have carried out research on the optimal configuration and operation of DES in distribution network. The study in [11] proposed a configuration method to jointly optimize the installation location, rated power and rated capacity of energy storage at the same time in order to prevent the voltage over-limit of low-voltage distribution network. The study in [12] constructed a two-layer optimization framework for DESS. The upper layer capacity allocation optimization model took the optimal investment economy after DESS was connected to the distribution network as the objective function, while the lower layer distribution point optimization model considered the efficiency of DESS in operation. The study in [13] took the measurement index of power network vulnerability, active power network loss and rated capacity of Energy Storage as targets, considered the coupling between planning and operation, and established the multi-objective siting capacity model of Energy Storage System (ESS), but the energy storage cost was not involved in the model. The study in [14] used affinity propagation (AP) clustering algorithm to divide the distribution network into multiple zones, and the clustering center node was selected to install ESS, and the capacity configuration of the hybrid energy storage system was carried out considering the charging and discharging efficiency of ESS and the state of SOC. However, the impact of the lack of DES participation in operation was not considered to improve the voltage and loss of the distribution network. The study in [15] proposed an optimal allocation method of energy storage in distribution network based on local constraints and quantitative evaluation of overall flexibility, aiming at the problem of sharp fluctuations of net load caused by a large number of distribution networks accessing distributed power sources. The study in [16], energy storage distribution was optimized based on the node voltage comprehensive sensitivity analysis method, and the DES optimization planning model was established with the dual objectives of minimum comprehensive cost and minimum voltage fluctuation sum of distribution network. The study in [17] established a two-layer energy storage configuration optimization model, in which the upper layer aimed at the minimum energy storage investment and the maximum photovoltaic consumption, and the lower layer aimed at the minimum variance of net load, but the voltage was not considered in the model. However, the above

*Corresponding Author.
This work was funded by the Program of National Natural Science Foundation of China (61903264).

method does not fully consider the zoning characteristics of the distribution of over-limit nodes during the operation of LVDN distribution network containing High Proportion Distributed Photovoltaic (HPDPV), so further research is still needed.

Considering the voltage over-limit treatment of HPDPV LVDN, this paper puts forward the method of partition optimization allocation of DES. Firstly, LVDN is partitioned, and then a multi-objective optimization model is established to determine the configuration nodes and capacity of DES. Finally, the actual low voltage network is taken as an example to verify the effectiveness of the proposed method.

II. LVDN Partitioning Method Based on K-means Clustering Algorithm

At present, there are two main installation methods of distributed energy storage, one is decentralized, but this method will make the installed energy storage too much, which will lead to uneconomical. The other is centralized, but this method will require very high communication conditions. Therefore, this paper uses K-means clustering algorithm, combined with the grid structure of LVDN, and based on the node voltage of the distribution line at the maximum load day and all day, the distribution line is divided into nodes.

A. Sample Data

In this paper, the node voltage of distribution line running at maximum load every day is taken as sample data. Suppose that the total number of independent nodes in the distribution network is N, the total number of nodes is N+1, the total number of branches is b, the branches n (m, n), the first node number is m, the last node number is n, and $n>m$, n =1, ..., N.

B. LVDN Partition

K-means clustering algorithm can classify data with high similarity into one class. It is very sensitive to noise and outliers and needs to specify the number of sets before running. Too large or too small a number of sets will affect the final result. In this paper, the elbow method is used to determine the number of center points, and the judgment index is the Sum of Squared Errors (SSE). Its basic principle is to draw the SSE curve of different cluster numbers with the change of k value, and find the "inflection point" where SSE quickly slows down, namely the position of the elbow. The k value corresponding to that position is the most reasonable value for the number of sets. SSE formula is as follows:

$$SSE=\sum_{i=1}^{k}\sum_{x\in C_i}\left\|x-\gamma_i\right\|_2^2 \tag{1}$$

where, C_i is the i set; γ_i is the set center of C_i.

The LVDN partitioning process based on K-means clustering algorithm is shown in Fig. 1, and the operation steps are as follows:

1) The elbow method is used to process the sample data and determine the number value of the set center k;

2) Calculate the distance between other data points and the center vector of the set and assign it to the set with the closest distance;

3) Update the center vector of the set;

4) If the center vector of the set changes, repeat step 2) and step 3), no change, go to step 5);

5) Output clustering results.

The flow chart is shown in Fig. 1.

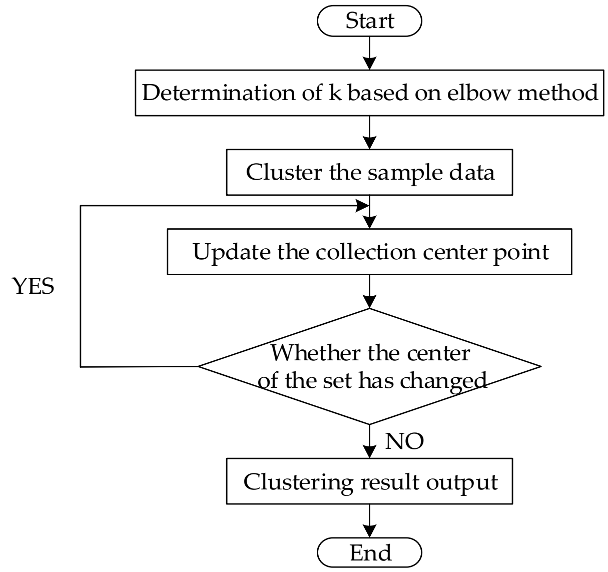

Fig. 1. Flow chart of *K*-means clustering algorithm.

III. DES Multi-Objective Optimization Model

In this chapter, DES multi-objective optimization model is established, including objective function and constraints. Then the multi-objective is normalized and the weight coefficient of the multi-objective is determined, so that the multi-objective is transformed into a single objective.

A. Objective Function

In order to reflect the improvement of distribution network operation state after DES optimal configuration, this paper takes improving node voltage, reducing power loss and minimizing the comprehensive cost of energy storage investment as the objective function.

1) Node voltage improvement degree: The improvement degree of node voltage is described by the decreased value of node voltage offset of distribution network before and after the optimal configuration of DES. The model expression is as follows:

$$\min f_1^{'}=\sum_{t=1}^{24}\sum_{i\in\Omega}\left(\frac{\left|U_{t.i}^{(1)}-U_{\mathrm{N}}\right|}{U_{\mathrm{N}}}-\frac{\left|U_{t.i}^{(0)}-U_{\mathrm{N}}\right|}{U_{\mathrm{N}}}\right)\times 100\% \tag{2}$$

where, Ω is the node set of distribution network; $U_{t,i}^{(0)}$ and $U_{t,i}^{(1)}$ are respectively the voltage of node i at time period t before and after DES is optimized.

2) Power loss: After optimizing the configuration of DES, the power loss of the distribution net-work is minimal:

$$\min f_2^{'}=\sum_{t=1}^{24}\sum_{l=1}^{b}3\times 10^{-3}\times I_l^2 R_l t \tag{3}$$

where, I_l is the current of branch l, A; R_l is the current of branch l, Ω; b is the number of branches.

2) DES comprehensive investment expenses: DES comprehensive investment cost mainly includes installation cost and operation and maintenance cost [18]. The objective function formula is as follows:

$$\min f_3^{'} = (C_{\mathrm{IC}} + C_{\mathrm{OMC}})\ P_{\mathrm{ess.instal}} \tag{4}$$

where, C_{IC} is the installation cost per unit power of the energy storage battery, calculated according to Eq. (5), yuan; C_{OMC} is the operation and maintenance cost per unit power of the energy storage battery, calculated according to Eq. (6), yuan; $P_{\mathrm{ess.instal}}$ is the total installed power of DES, kW.

$$C_{\mathrm{IC}} = (C_{\mathrm{S}}\frac{t_{\mathrm{n}}}{\eta} + C_{\mathrm{P}} + C_{\mathrm{AF}}t_{\mathrm{n}})\frac{r(1+r)^N}{(1+r)^N - 1} \tag{5}$$

where, r is the depreciation rate; N for the use of cycle life; C_{S} is the unit energy price of the battery body (yuan /(kWh)); C_{P} is the unit power price of two-way energy conversion equipment (yuan/kW); C_{AF} is the unit energy price of auxiliary equipment (yuan /(kWh)); t_{n} is the rated charging and discharging time of the energy storage battery, h.

$$C_{\mathrm{OMC}} = C_{\mathrm{O\_P}} + C_{\mathrm{C}}\frac{t_{\mathrm{n}}}{\eta}T \tag{6}$$

where, $C_{\mathrm{O\_P}}$ is the basic operation and maintenance cost per unit power of the energy storage battery (yuan/kW); C_{C} is the charging electricity price (yuan/(kWh)); T indicates the number of operating days per year.

B. Constraint Condition

In order to maintain the stable operation of LVDN, the optimized allocation model of energy storage partition constructed must meet the following constraints.

1) Power balance constraint: The model satisfies the following power balance constraints [19]:

$$\begin{cases} P_{\mathrm{G}i} + P_{\mathrm{pv}i} - P_{Li} \pm P_{\mathrm{ess}} = U_i\sum_{j=1}^{N}U_j(G_{ij}\cos\theta_{ij} + B_{ij}\sin\theta_{ij}) \\ Q_{\mathrm{G}i} + Q_{\mathrm{pv}i} - Q_{Li} \pm Q_{\mathrm{ess}} = U_i\sum_{j=1}^{N}U_j(G_{ij}\sin\theta_{ij} - B_{ij}\cos\theta_{ij}) \end{cases} \tag{7}$$

where, $P_{\mathrm{G}i}$ and $P_{\mathrm{pv}i}$ are the active power injected by the system and DPV into node i, kW; $Q_{\mathrm{G}i}$ and $Q_{\mathrm{pv}i}$ are the reactive power injected into node i by the system and DPV, kvar; $P_{\mathrm{L}i}$ is the active power consumed by node i, kW; $Q_{\mathrm{L}i}$ is the reactive power consumed by node i, kvar; P_{ess} is the active power absorbed or emitted by ESS, kW; Q_{ess} is reactive power absorbed or emitted by ESS, kvar.

2) Nodal voltage constraint: After the configuration of DES, the LVDN node with a high proportion of distributed PV voltage offset does not exceed ±5%, namely:

$$-5\% \le \frac{U_i - U_{\mathrm{N}}}{U_{\mathrm{N}}} \times 100\% \le 5\% \tag{8}$$

3) Energy storage battery confinement: The regulation of energy storage battery has bidirectional effectiveness, and the constraint formula is:

$$-1 \le \varepsilon(d,t) \le 1 \tag{9}$$

where, ε (d, t) is the power adjustment function.

SOC of energy storage battery has upper and lower limits, and the constraint formula is [20]:

$$\mathrm{SOC}_{\min} \le \mathrm{SOC}(t) \le \mathrm{SOC}_{\max} \tag{10}$$

4) DPV constraint: The output power and total installed capacity of DPV must meet the constraints shown in Eq. (11) and Eq. (12) respectively.

$$0 \le P_{\mathrm{PV}} \le P_{\mathrm{PV\max}} \tag{11}$$

where, PPV is the active power output of DPV, kW; PPVmax is the maximum output power of DPV, kW.

$$P_{\mathrm{PV.instal\,min}} \le P_{\mathrm{PV.instal}} \le P_{\mathrm{PV.instal\,max}} \tag{12}$$

where, $P_{\mathrm{PV.instal\ min}}$ is the minimum active component of the total installed capacity of DPV, kW; $P_{\mathrm{PV.instal\ max}}$ indicates the maximum active power component of the total installed DPV capacity, kW.

5) Line current constraint: The model satisfies the following line current constraint:

$$I_{l\min} \le I_l \le I_{l\max} \tag{13}$$

where $I_{l\min}$ is the lower limit of line current, A; I_l is the line current value, A; $I_{l\max}$ is the upper limit of line current, A.

C. Normalization of Multiple Objective Functions

In order to determine the location and capacity of DES site selection, the objective function is normalized, and the weight coefficient is allocated to the objective function, and the multi-objective function is changed into a single objective function.

The objective function is normalized [21] as follows:

$$\begin{cases} f_1 = \dfrac{f_1^{'} - f_{1\ \min}^{'}}{f_{1\ \max}^{'} - f_{1\ \min}^{'}} \\ f_2 = \dfrac{f_2^{'} - f_{2\ \min}^{'}}{f_{2\ \max}^{'} - f_{2\ \min}^{'}} \\ f_3 = \dfrac{f_3^{'} - f_{3\ \min}^{'}}{f_{3\ \max}^{'} - f_{3\ \min}^{'}} \end{cases} \tag{14}$$

where, $f'_{1\ \min}$ and $f'_{1\ \max}$ are respectively the minimum and maximum values of the first objective function; $f'_{2\ \min}$ and $f'_{2\text{-}\max}$ are respectively the minimum and maximum values of the second objective function; $f'_{3\ \min}$ and $f'_{3\ \max}$ are respectively the minimum and maximum values of the third objective function.

The multi-objective function is transformed into a single objective function, as follows:

$$\min F = \omega_1 f_1 + \omega_2 f_2 + \omega_3 f_3 \tag{15}$$

where, ω_i is the weight coefficient of multiple objective functions (i =1,2,3), 0< ω_i <1 and $\omega_1+\omega_2+\omega_3=1$.

D. Determination of Weight Coefficients of Multiple Objective Functions

The analytic Hierarchy Process (AHP) is adopted to define the weight of the objective function by constructing a judgment matrix. Table I is the element judgment table, and the scale in the table is used to prioritize the targets.

TABLE I. ELEMENT SCALE JUDGMENT TABLE

Scale	Meaning
1	Equally important
3	The former is slightly more important than the latter
5	The former is significantly more important than the latter
7	The former is more important than the latter
9	The former is the most important
2、4、6、8	Represents the median value of the above adjacent judgments
The reciprocal of 1 to 9	Represents the importance of the exchange order comparison of the corresponding two factors

According to the judgment elements, the corresponding judgment matrix K is formed:

$$K = \begin{bmatrix} a_{11} & a_{12} & \cdots & a_{1n} \\ a_{21} & a_{22} & \cdots & a_{2n} \\ \vdots & \vdots & \ddots & \vdots \\ a_{n1} & a_{n2} & \cdots & a_{nn} \end{bmatrix} \tag{16}$$

where, a is the scale value obtained according to the element judgment table, where a_{ij} and a_{ji} are reciprocal of each other; n represents the number of optimization objectives.

The root method is used to calculate the weight of the optimization objective, and the calculation formula is as follows:

$$\begin{cases} \varpi_i = \sqrt[n]{\prod_{j=1}^{n} a_{ij}} \\ \omega_i = \dfrac{\varpi_i}{\sum_{j=1}^{n} \varpi_j} \end{cases} \tag{17}$$

where, ϖ_i is the geometric mean value of a_{ij}; ω_i is the weight coefficient of the optimization objective.

Finally, consistency test is carried out to illustrate the rationality of the weight determination method. The calculation formula is as follows:

$$\begin{cases} C_1 = \dfrac{\lambda_{\max} - n}{n-1} \\ C_R = \dfrac{C_1}{R_1} \end{cases} \tag{18}$$

where, C_1 is a consistency index to measure the degree of inconsistency; R_1 is the given random consistency index; $\lambda_{\max}$ is the largest characteristic root; C_R is the judgment value of test results. When $C_R<0.1$, it indicates that the weight coefficient is selected reasonably.

IV. MULTI-OBJECTIVE OPTIMIZATION MODEL SOLVING BASED ON WHALE ALGORITHM

In this paper, whale algorithm is used to solve the model. The advantages of this algorithm are that it is simple to operate, requires fewer parameters, and has strong ability to jump out of local optimization.

A. Overview of Whale Algorithm Principles

Whale Optimization Algorithm (WOA) simulates the cooperation and competition among individuals in the humpback whale population, and uses adaptive search strategy to find the optimal solution of the objective function efficiently. WOA consists of three stages: encircling predation phase, bubble attack phase, and random hunting phase [22].

1) Encircling predation phase: It can be assumed that the current optimal search agent is the target prey or close to the target prey, and other search agents will update the location of the best search agent in order to find the optimal solution faster. This search strategy can avoid falling into the local optimal and unable to continue optimization [23]. The formula is as follows:

$$\vec{D} = \left| \vec{C} \cdot \vec{X}^*(t) - \vec{X}(t) \right| \tag{19}$$

$$\vec{X}(t+1) = \vec{X}^*(t) - \vec{A} \cdot \vec{D} \tag{20}$$

where, $\vec{X}(t)$ is the position vector of the current search agent; $\vec{X}^*(t)$ is the position vector of the current best search agent, which changes with the number of iterations; t is the number of iterations; $\vec{A}$ and $\vec{C}$ are coefficient vectors.

Among them:

$$\vec{A} = 2\vec{a} \cdot \vec{r} - \vec{a} \tag{21}$$

$$\vec{C} = 2\vec{r} \tag{22}$$

$$a = 2 - \frac{2t}{T_{\max}} \tag{23}$$

where, $\vec{r}$ is a random vector with a value range of [0, 1]; $\vec{a}$ is the parameter control vector, and the value decreases linearly from 2 to 0 in the algorithm iteration process; $T_{\max}$ is the upper limit of the number of algorithm iterations.

2) Bubble attack phase: There are two strategies in the bubble attack phase, which are contraction encir-cling mechanism and spiral update position. Among them, the shrinkage enveloping mechanism is realized by changing the value of parameter a, and there is a linear relationship between parameter a and A. With the strategy of spiral update position, the whale optimization algorithm can search the space more comprehensively, so as to find the potential optimal solution better. The position of spiral update is shown in Fig. 2.

The formula for calculating spiral update position is as follows:

$$\vec{X}(t+1) = \vec{D} \cdot e^{bl} \cdot \cos(2\pi l) + \vec{X}^{*}(t) \tag{24}$$

where, $\vec{D}$ is the distance between the search agent and the optimal search agent location; b is the constant controlling the update of spiral position; l is the random number of [-1, 1].

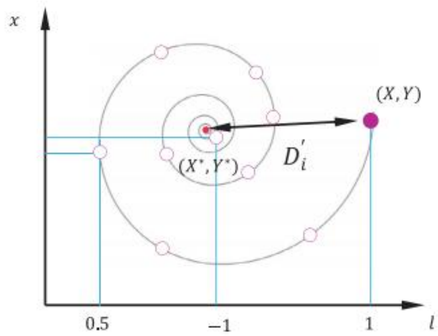

Fig. 2. Position of spiral update.

In the bubble attack phase, humpbacks tend to do both at the same time. To simulate this synchronous behavior, the humpback was assumed to have a 50% chance of choosing to use one of the two methods. When probability p<0.5, humpback whales will choose to use shrinkage encircling mechanism, otherwise they will use spiral up-date position method, in order to update their position during optimization, the formula is as follows:

$$\vec{X}(t+1) = \begin{cases} \vec{X}^{*}(t) - \vec{A} \cdot \vec{D}, p < 0.5 \\ \vec{D} \cdot e^{bl} \cdot \cos(2\pi l) + \vec{X}^{*}(t), p \geq 0.5 \end{cases} \tag{25}$$

3) Random hunting phase: The whale position is changed by coefficient A. When $|\vec{A}|$ is greater than 1, the search agent is forced to move away from the reference optimal position, and the whale will randomly search for food in the global scope, effectively avoiding the dis-advantage of local optimal [24]. The formula for this stage is as follows:

$$\vec{D} = \left| \vec{C} \cdot \vec{X}_{rand} - \vec{X}(t) \right| \tag{26}$$

$$\vec{X}(t+1) = \vec{X}_{rand} - \vec{A} \cdot \vec{D} \tag{27}$$

where, $\vec{X}_{rand}$ randomly selects an individual whale and takes its position vector as the reference vector.

B. Whale Algorithm Solution Process

The WOA operation steps are as follows:

1) Initialize population number and iteration times, and set relevant parameters;

2) Each search agent performs iterative optimization in accordance with the three stages in WOA, and then updates the optimal value of the best search agent and the optimal position vector according to the fitness values of the search agent, the best search agent and the reference search agent, and saves records at the same time;

3) Judge whether the WOA program meets the termination requirement, if so, output the result, otherwise, perform step 2);

4) Output the best search agent position vector of the last iteration.

The WOA process is shown in Fig. 3 (shown at the end of this paper).

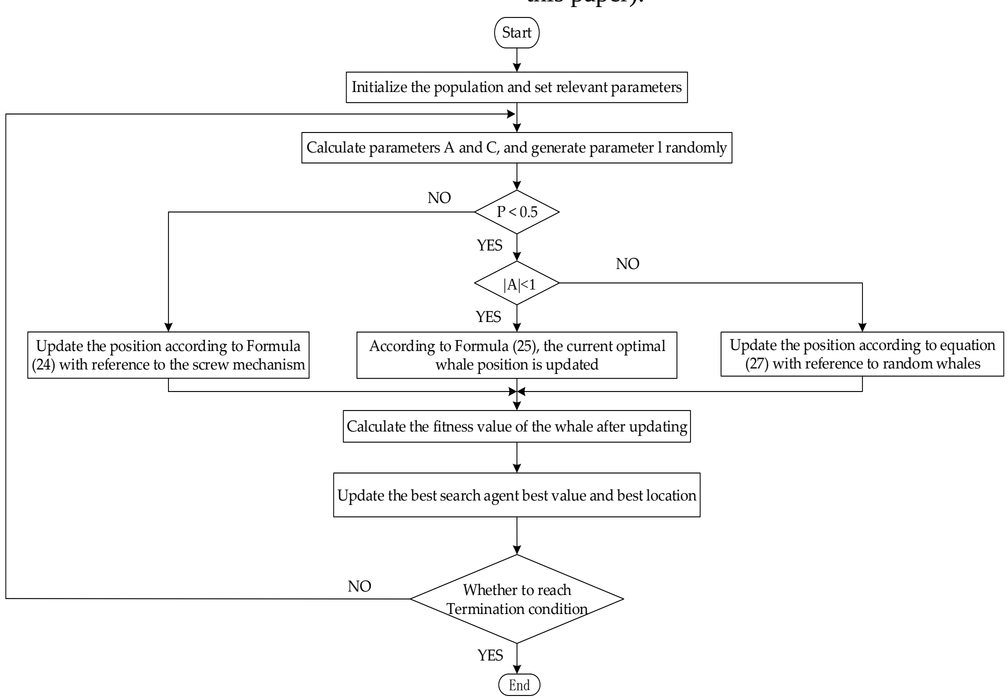

Fig. 3. Flow chart of whale algorithm.

V. Example Analysis

A. Example Introduction

Take an actual low-voltage network as an example, as shown in Fig. 4, N=46, b=46, 0~46 are node numbers, node 0 is the reference node, and its voltage remains unchanged to $1.05U_N$. The district has 1 non-industrial user, 191 residential lighting households, 4 agricultural production households and 1 commercial electricity consumption household. The proportion of DPV connected to LVDN is set to 100%. It is assumed that each household has the same photovoltaic capacity and the photovoltaic output is basically the same. The maximum and minimum load curves of the system are shown in Fig. 5.

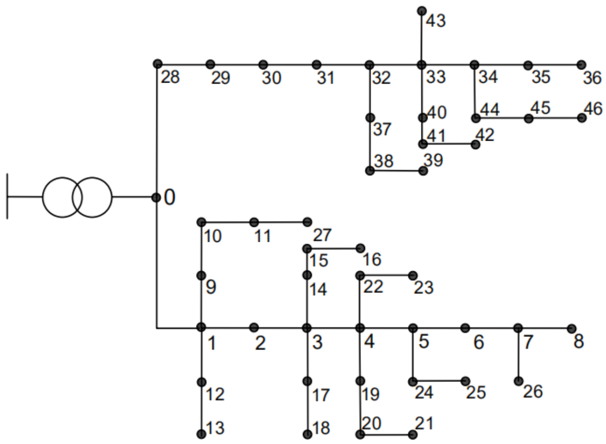

Fig. 4. 0.38kV radiant network diagram.

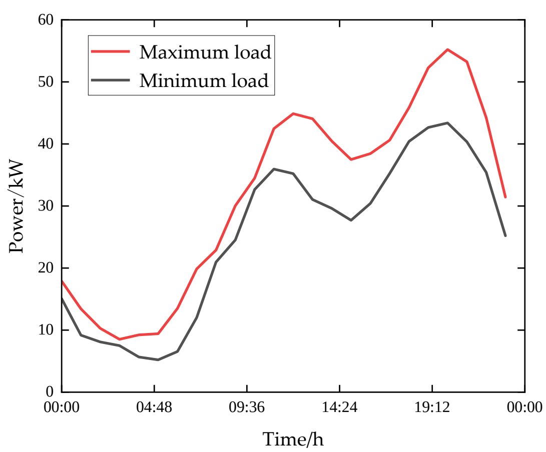

Fig. 5. Maximum / minimum load curve.

B. Partition Results

After calculating the 24-hour node voltage distribution of the maximum load day of the system shown in Fig. 4, the K-means clustering algorithm is used to cluster and partition the distribution network nodes. Fig. 6 is the change diagram of the SSE curve. It can be seen from Fig. 6 that the SSE turning point appears around k=10, and when k exceeds 10, the change range of SSE is very small. Therefore, the set center number of K-means clustering algorithm is 10. The system shown in Fig. 4 is divided into 10 types of partitions, as shown in Fig. 7. Table II shows the node numbers contained in the distribution network partitions. Each type of partition, the energy storage device is configured to regulate the node voltage.

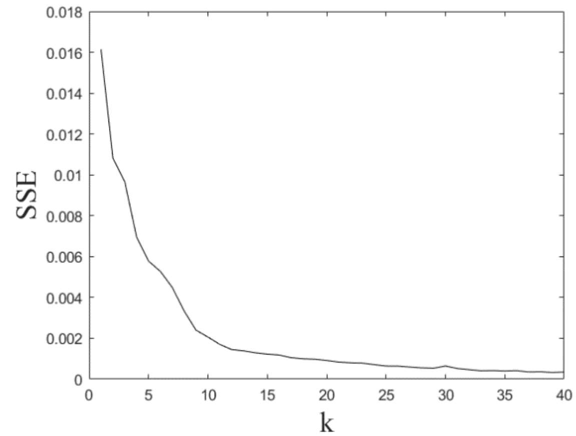

Fig. 6. SSE variation curve.

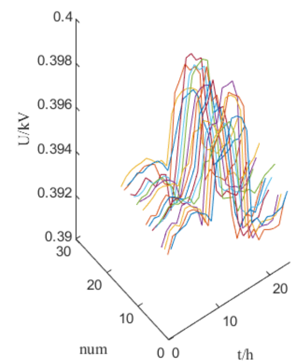

(a) cluster partition type 1

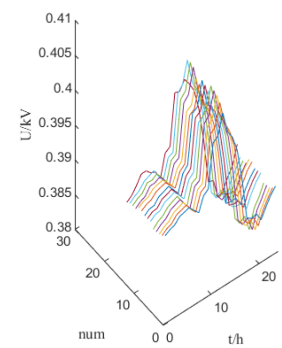

(b) cluster partition type 2

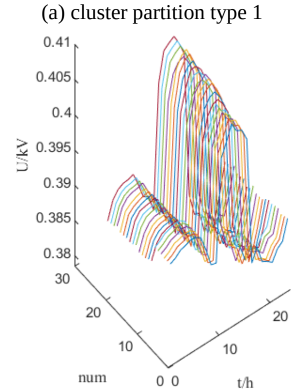

(c) cluster partition type 3

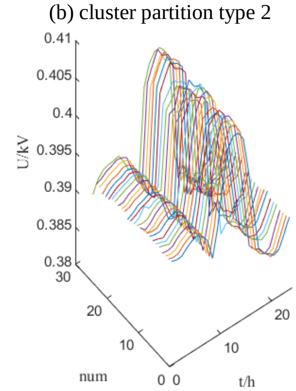

(d) cluster partition type 4

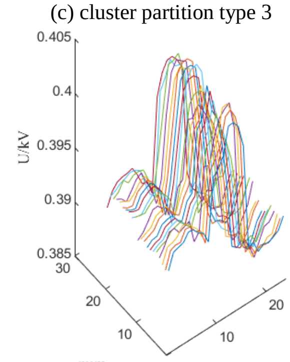

(e) cluster partition type 5

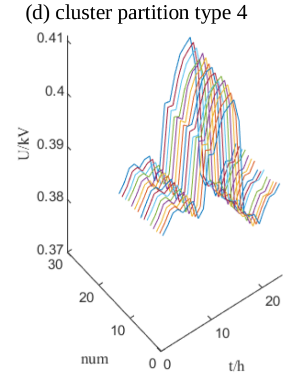

(f) cluster partition type 6

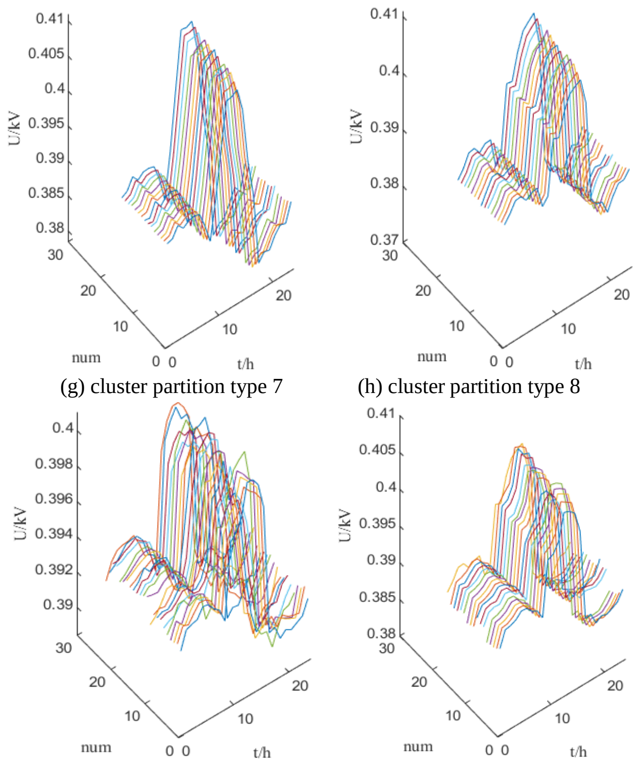

(g) cluster partition type 7 (h) cluster partition type 8

(i) cluster partition type 9 (j) cluster partition type 10

Fig. 7. Distribution network node clustering partitions.

TABLE II. DISTRIBUTION NETWORK NODE ZONES WEIGHT COEFFICIENTS OF OPTIMIZATION OBJECTIVES

Partition number	Number of a node in a zone
1	34, 35, 36, 44, 45, 46
2	4, 5, 22, 23, 24, 25
3	1, 2, 3, 12, 13, 17, 18
4	33, 40, 41, 42, 43
5	28, 29, 30, 31
6	9, 10, 11, 27
7	6, 7, 8, 26
8	19, 20, 21
9	14, 15, 16
10	32, 37, 38, 39

C. Optimization Scheme and Result Analysis

1) Optimization scheme: The weight coefficients of optimization objectives determined by AHP are shown in Table III, and the test results are shown in Table IV. According to Table III and Table IV, the weight coefficient of optimization objective determined by AHP passes the test.

TABLE III. WEIGHT COEFFICIENTS OF OPTIMIZATION OBJECTIVES

Optimization objective	Weight coefficient
Node voltage improvement degree f_1	0.6267
Power loss f_2	0.2797
Comprehensive cost f_3	0.0936

TABLE IV. CONSISTENCY TEST RESULTS

Maximum characteristic root	C_1	R_1	C_R	Consistency test result
3.0858	0.0429	0.525	0.0817	Pass

In this paper, the active power component of a single distributed battery capacity is not more than 60 kWh. The related parameters of energy storage battery installation cost are as follows: depreciation rate r=10%; Service cycle life N=10 years; Battery body unit energy price C_S=3720 yuan; Unit power of two-way energy conversion equipment C_P=1085 yuan; Unit energy C_{AF} of auxiliary facilities is 186 yuan; The rated charging and discharging time of the energy storage battery t_n=12h; The basic operation and maintenance cost of energy storage battery per unit power C_{O_P}=124 yuan, charging electricity price C_C=0.5 yuan; Equivalent annual operating days T=180 days. Before the DES battery is connected, the peak load of 47-node radiant LVDN system is 749.04kW. After 100% DPV is connected, the maximum node voltage offset is 8.2%, and the maximum DES comprehensive installation cost C_{max}=1,000,000 yuan. Based on MATLAB software, WOA was used to optimize the configuration of DES batteries in the system shown in Fig. 4. The number of population in WOA is 100 and the maximum number of iterations is 100. The optimization scheme is shown in Table V.

TABLE V. THE DES OPTIMIZATION SCHEME

Partition number	DES Indicates the number of the con-figuration node	DES configuration capacity(kWh)
1	44	50
2	24	40
3	17	60
4	43	50
5	30	50
6	10	60
7	7	40
8	20	50
9	15	60
10	38	30

2) Optimization scheme: The maximum daily load and minimum daily load of LVDN in a year are selected to verify whether the DES planning scheme meets the actual demand of LVDN. The comparison of optimization results is shown in Table VI.

TABLE VI. COMPARISON OF OPTIMIZATION RESULTS

Type	Sum of absolute value of node voltage offset		Power loss of distribution network (kWh)	
	Minimum load	Maximum load	Minimum load	Maximum load
Before optimization	3.1093	4.3179	14.1896	16.2202
After optimization	1.9026	2.147	6.0169	6.7923

Fig. 8 shows the three-dimensional comparison diagram of voltage offset of distribution network nodes before and after optimization. In order to clearly and effectively illustrate the optimization effect, typical nodes are selected for further analysis, as shown in Fig. 9.

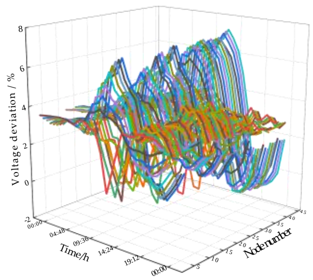

(a) Three-dimensional comparison of voltage shift curve at max load node.

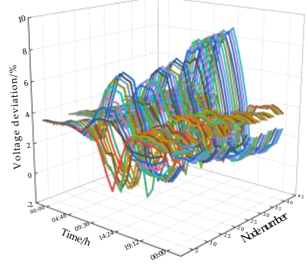

(b) Three-dimensional comparison of voltage shift curve at min load node.

Fig. 8. Node voltage offset curves before and after optimization three-dimensional contrast figures.

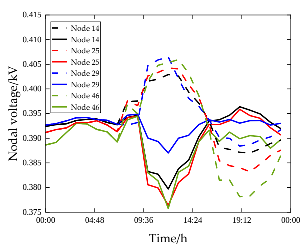

(a) Maximum load node voltage curve comparison.

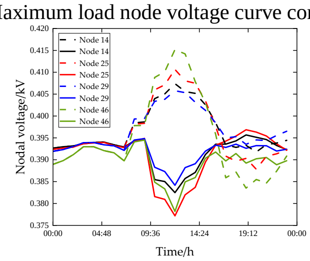

(b) Minimum load node voltage curve comparison.

Fig. 9. Comparison of node voltage before and after optimization.

In Fig. 9, dashed lines represent voltage curves of typical LVDN nodes before optimization, while solid lines represent voltage curves of typical LVDN nodes after optimization. As can be seen from Fig. 9, when LVDN is at the maximum daily load or minimum daily load, the DES optimal configuration scheme can play a good role, and the node voltage of the distribution network is below 1.05U_N. During the peak of DPV output, the connection of DES effectively reduces the node voltage and avoids the occurrence of node voltage overshoot.

Table VII compares the maximum node voltage offset before and after the maximum load optimization with the minimum load optimization. It can be seen from Table VII that the maximum node voltage offset before the maximum load optimization is 7.2%, after the optimization is 4.71%, before the minimum load optimization is 8.5%, and after the optimization is 4.49%.

TABLE VII. COMPARISON OF VOLTAGE OFFSETS BEFORE AND AFTER MAX/MIN LOAD OPTIMIZATION

Parse	Load condition	Maximum node voltage offset (%)
Before optimization	Maximum load	7.2
	Minimum load	8.5
After optimization	Maximum load	4.71
	Minimum load	4.49

According to Fig. 8, Fig. 9, Table VI and Table VII, the DES optimal configuration method proposed in this paper can improve the node voltage over-limit phenomenon, reduce the node voltage fluctuation, and make the LVDN node voltage curve smoother.

Fig. 10 shows the comparison of LVDN branch active power loss before and after optimizing DES configuration, where the dotted line represents before optimization and the solid line represents after optimization. According to Fig. 10 and Table VI, LVDN active power loss decreased significantly after optimal configuration of DES. Under the maximum load, the active loss of distribution network branch decreased from 16.2202kW to 6.7923kW, and under the minimum load, the active loss of distribution network branch decreased from 14.1896kW to 6.0169kW.

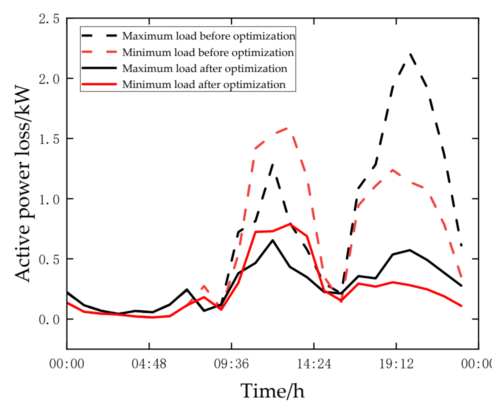

Fig. 10. Comparison of active power loss of distribution network branches before and after optimization.

VI. CONCLUSION

The optimal configuration of energy storage can effectively solve the problem of voltage exceeding limit caused by high proportion distributed photovoltaic. Considering the governance of LVDN node voltage overrun problem of HPDPV, this paper establishes a multi-objective optimization model for optimal configuration of DES, and uses whale algorithm to solve the model. Based on the actual case of a certain region, the effectiveness of the method is verified. The conclusions are as follows:

1) In LVDN containing HPDPV, the optimal configuration of DES can reduce the mismatch between the volatility of the photovoltaic power supply and the load characteristics, solve the voltage overrun problem, and reduce the node voltage fluctuation of LVDN.

2) Based on the node voltage of LVDN maximum load day and all day, the K-means clustering algorithm is used to partition LVDN and optimize the partition configuration of DES, which is conducive to HPDPV consumption.

3) When constructing the DES multi-objective optimal configuration model, taking improving the node voltage, reducing the power loss of the distribution network, and minimizing the comprehensive cost of energy storage investment as the objective function, considering the power balance, energy storage battery, and other constraints, the whale algorithm is used to determine the DES optimal configuration scheme, which is in line with the actual operation of LVDN.

Acknowledgment

This research was funded by the Program of National Natural Science Foundation of China (Grant number 61903264).

References

[1] Y. L. Li, L. Wei, J. T. Zhao, *et.al*, "Effect of distributed PV grid on voltage of distribution network," Journal of Power Sources, vol. 40, no. 6, pp. 1257-1259, 2016.

[2] Z. Y. Pei, J. Ding, C. Li, *et.al*, "Analysis and Suggestion for Distributed Photovoltaic Generation," Electric Power, vol. 51, no.10, pp. 80-87, 2018.

[3] Y, Chen, D. C. Liu, J. Wu, *et.al*, "Research on influence of distributed photovoltaic generation on voltage fluctuations in distribution network," Electrical Measurement & Instrumentation, vol. 55, no. 14, pp. 27-32, 2018.

[4] Q. Tao, B. Y. Sang, J. L. Ye, J. H. Xue, "Optimal Configuration Method of Distributed Energy Storage Systems in Distribution Network with High Penetration of Photovoltaic," High Voltage Engineering, vol. 42, no. 7, pp, 2158-2165, 2016.

[5] Z. Li, W. B. Wang, S. F. Han, L. J. Lin, "Voltage adaptability of distributed photovoltaic access to a distribution network considering reactive power support," Power System Protection and Control, vol. 50, no. 11, pp, 32-41. 2022.

[6] S. He, S. J. Lin, G. K. Li, "Multi-objective optimal allocation and operation of distributed energy storage in low-voltage distribution network with photovoltaic integration," Advanced Technology of Electrical Engineering and Energy, vol. 38, no. 3, pp. 18-27, 2019.

[7] Y. X. Xia, Q. S. Xu, Y. Huang, H. Y. Qian, "Optimal Configuration of Distributed Energy Storage for Distribution Network in Peer-to-peer Transaction Scenarios," Automation of Electric Power Systems, vol. 45, no. 14, pp. 82-89, 2021.

[8] H. Xiao, W. Pei, W. Deng, L. Kong, "Analysis of the Impact of Distributed Generation on Distribution Network Voltage and Its Optimal Control Strategy," Transactions of China Electrotechnical Society, vol. 31, pp. 203-213, 2016.

[9] M. N. Kabir, Y. Mishra, G. Ledwich, Z. Y. Dong, K. P. Wong, "Coordinated Control of Grid-Connected Photovoltaic Reactive Power and Battery Energy Storage Systems to Improve the Voltage Profile of a Residential Distribution Feeder," IEEE Trans. Industrial Informatics, vol. 10, no. 2, pp. 967–977, 2014.

[10] Y. F. Wang, X. W. Dong, F. Yang, *et.al*, "Optimal configuration of distributed energy storage system based on voltage quality of distribution network," Thermal Power Generation, vol. 49, no. 8, pp. 126-133, 2020.

[11] A. Giannitrapani, S. Paoletti, A. Vicino, D. Zarrilli, "Optimal Allocation of Energy Storage Systems for Voltage Control in LV Distribution Networks," IEEE Transactions on Smart Grid, vol. 8, no. 6, pp. 2859-2870, 2017.

[12] Y. L. Jia, Z. Q. Mi, L. Q. Liu, Q. K. Yin, "Comprehensive optimization method of capacity configuration and ordered installation for distributed energy storage system accessing distribution network," Electric Power Automation Equipment, vol. 39, no. 4, pp. 1-7, 2019.

[13] Q. M. Yan, X. Z. Dong, J. H. Mu, Y.X. Ma, "Power System Protection and Control," Power System Protection and Control, vol. 50, no. 10, pp. 11-19, 2022.

[14] H. T. Liu, L. Xu, S. P. Hao, *et.al*, "Optimization method of distributed hybrid energy storage based on distribution network partition," Electric Power Automation Equipment, vol. 40, no. 5, pp. 137-145, 2020.

[15] X. R. Zhu, G. W. Lu, "Optimal allocation of energy storage systems considering flexibility in distribution network," Modern Electric Power, vol. 37, no. 4, pp. 341-352, 2020.

[16] J. M. Zhao, J. Y. Su, F. Pan, et.al, "Dual objective optimization planning of distributed energy storage for active distribution network considering photovoltaic fluctuations," Renewable Energy Resources, vol. 40, no. 11, pp. 1546-1553, 2022.

[17] X. Liu, X. F. Ning, Y. Jin, *et.al*, "A hierarchical optimal configuration method for distributed energy in distribution networks," Zhejiang Electric Power, vol. 42, no. 5, pp. 95-104, 2023.

[18] J. H. Xue, J. L. Ye, Q. Tao, *et.al*, "Economic Feasibility of User-Side Battery Energy Storage Based on Whole-Life-Cycle Cost Model," Power System Technology, vol. 40, no. 8, pp. 2471-2476, 2016.

[19] F. F. Zheng, X. F. Meng, T. F. Xu, *et.al*, "Optimization Method of Energy Storage Configuration for Distribution Network with High Proportion of Photovoltaic Based on Source–Load Imbalance," Sustainability, vol. 15, pp. 10628, 2023.

[20] F. F. Zheng, X. F. Meng, T. F. Xu, *et.al*, "Voltage Zoning Regulation Method of Distribution Network with High Proportion of Photovoltaic Considering Energy Storage Configuration," Sustainability, vol. 15, pp. 10732, 2023.

[21] W. R. Pan, Z. Wei, Q. Sun, *et.al*, "Collaborative Optimal Strategy of Electric Vehicles and Wind Power with the consideration of Electricity Price Optimization," Electrotechnics Electric, vol. 6, pp. 14-21+38, 2023.

[22] J. Sun, Z. C. Yu, "The fault self-healing strategy of distribution network system with distributed energy storage system considering load demand response," Engineering Journal of Wuhan University, pp. 1-15, 2023.

[23] L. Q. Hang, M. Liu, "Multi-Objective Optimization Configuration of Synchronized Phasor Measurement Units Based on Improved Whale Optimization Algorithm," Modern Electric Power, pp. 1-8, 2023. DOI: 10.19725/j.cnki.1007-2322.2022.0276.

[24] L. L. Xu, C. Yang, H. R. Zeng, "Fault section location of distribution network with DG based on improved whale algorithm," Electronic Science and Technology, vol. 36, no. 1, pp. 15-20+27, 2023.